A STUDY ON THE STRUCTURAL RELATIONSHIP BETWEEN BLEOMYCIN ANALOGS AND DNA HAIRPINS

Undergraduate Thesis

Presented to the Honors College at the

University of Wyoming in Partial

Fulfillment of the Requirements for the

University Honors Program

By

Sally A. Murray

Mentor: Dr. Teresa Lehmann

Laramie, Wyoming

December 2017

Research Story: I became involved with the following research on bleomycin analogs and DNA hairpins, after responding on a whim to a campus-wide email regarding a research position in the chemistry department. It has been roughly four years since I was hired by Dr. Teresa Lehmann to begin work on the project, in which time we have published three papers. As an undergraduate researcher I came to be involved in all aspects of the scientific process. For the research that is to be discussed herein, I was involved in the experimental design, sample preparation and data collection, as well as the analysis of complex two-dimensional NMR spectra. I also participated in the writing of the three papers and the presentation of our research at various seminar talks. Throughout my time as an undergraduate researcher, I witnessed the ways in which scientific endeavors can make a positive difference in society. This project specifically elucidates a complicated DNA:Drug interaction which had been previously under controversy due to inconsistencies within the field regarding experimental design. Ultimately, we produced results that could be used to guide the development of a more effective, and less toxic anticancer drug.

The following is to be a summary of the research I conducted while in the Lehmann group, including a reflection on how my involvement in this project has contributed to my identity at the University of Wyoming and beyond.

Introduction: Bleomycins (BLMs) are a class of glycopeptide-derived antibiotics that are isolated from *Streptomyces verticillus* [1]. Their structures are comprised of four different functional domains related to metal binding, DNA binding, and cell-surface recognition [2]. A fourth domain, referred to as the linker region, promotes a compact, bent conformation [2]. In its active form, the drug mediates a sequence selective, metal dependent oxidative cleavage of DNA [3]. To this end, BLM has been used to cleave DNA at sites of cancerous cell growth. As a chemotherapeutic agent,

BLM has been used to treat squamous cell carcinomas [4], non-Hodgkin's lymphomas [5], testicular carcinomas [6], and ovarian cancers [7].

A side effect commonly associated with BLM treatment is pulmonary fibrosis, which causes scarring in the lungs that can interfere with the patient's breathing and sometimes be fatal. Interestingly, different degrees of pulmonary fibrosis have been linked to different types of BLM, with BLM-B_2 and Pep being reportedly less toxic than BLM-A_2 and BLM-A_5 [8-18]. Analogs of BLM are differentiated from one another by their unique C-terminal substituent, referred to as the "tail". Due to the fact that the C-terminus is involved in DNA binding [19-30], it is tempting to consider that variation in the tail could cause changes in the DNA-BLM complex that could relate to the different degrees of toxicity observed for the various forms of the drug.

To date, research on the interaction between BLM and DNA has been conducted using different combinations of DNA fragments, BLMs, and metal-centers [19-30]. While the results of these studies have led to the proposal of the three different modes of binding [22, 24, 26, 30], they have disregarded the potential relationship between the C-termini and the variable intermolecular interactions that are observed for the different BLM-DNA complexes. In this way, there is not a clear connection between any of the variables being manipulated and the structural differences that are observed upon binding.

Our research effectively isolates two variables, the DNA fragment and the BLM, in order to elucidate their structural relationship and provide consistency and comparability within our field. We use nuclear magnetic resonance (NMR) spectroscopy to gain the most detailed image of these interactions. Ultimately, we arrive at the interesting conclusion that of the two preferential DNA binding sites (5'-GC-3' *vs.* 5'-GT-3') one is more preferred. Also, we show that, depending

on which BLM is bound, the structure of both the DNA and the drug change differently, which could perhaps be related to the aforementioned toxicity spectrum.

Bleomycin Structure: As mentioned previously, the BLM structure can be divided into four different functional domains (Figure 1). First, the metal binding domain, which consists of the β-aminoalanine, pyrimidinylpropopnamide, and β-hydroxyhistidine moieties; provides the ligands for metal complexation and O_2 activation [31-33]. BLM requires a metal ion cofactor in order to cleave DNA [34-36]. Specifically, in vivo, the drug binds Fe^{2+} to form the biologically active form of the complex, where in the presence of activated molecular oxygen DNA is cleaved. Other inactive forms of bleomycin exist; these include Zn^{2+} [22, 38-41] and Co^{3+} [42, 43] complexes which induce proper folding of the drug without activating oxygen or cleaving DNA. Separately, the metal binding domain has also been reported as contributing to DNA binding and being necessary for sequence selectivity [31-33].

The DNA binding domain includes the bithiazole moiety and the variable C-terminal substituent. DNA is bound to BLM via hydrophobic interactions involving the bithiazole moiety, and electrostatic interactions between the negatively charged DNA phosphate backbone and positively charged C-terminal substituent [44-47]. Based on these types of connections, three different modes of binding have been proposed. Two of these involve the partial [24, 26] and total [30] intercalation of the bithiazole unit between DNA bases. A third mode of binding suggests that the drug binds to the minor groove of the DNA [22]. Previous studies show that the type of binding may depend on the target DNA sequence. For example, binding at the minor groove dominates for AT-rich DNA sequences, while binding via intercalation is specific to GC DNA sequences. Ultimately, BLM has two preferred DNA-binding sites, 5'-GC-3' and 5'-GT-3', and four

variations of the C-terminal substituent, whose structures are referred to as -A_5, -A_2, -B_2, and peplomycin (PEP). As such, the combination of the DNA binding site and the C-terminal substituent determine the mode of binding and the resultant interactions.

The region between the metal binding and DNA binding domains is called the linker, and consists of the methylvalerate (Val) and threonine (Thr) moieties. This region promotes a compact, bent conformation that allows for interaction between the metal binding and DNA binding domains with DNA, ultimately facilitating an efficient DNA cleavage event [48].

Lastly, the disaccharide domain contains the α-L-gulose (Gul) and α-D-mannose (Mann) moieties. These are involved in cell-surface recognition and cellular uptake, perhaps to be involved in tumor-targeting [49]. It has also been reported that this domain contributes to metal-ion coordination [50].

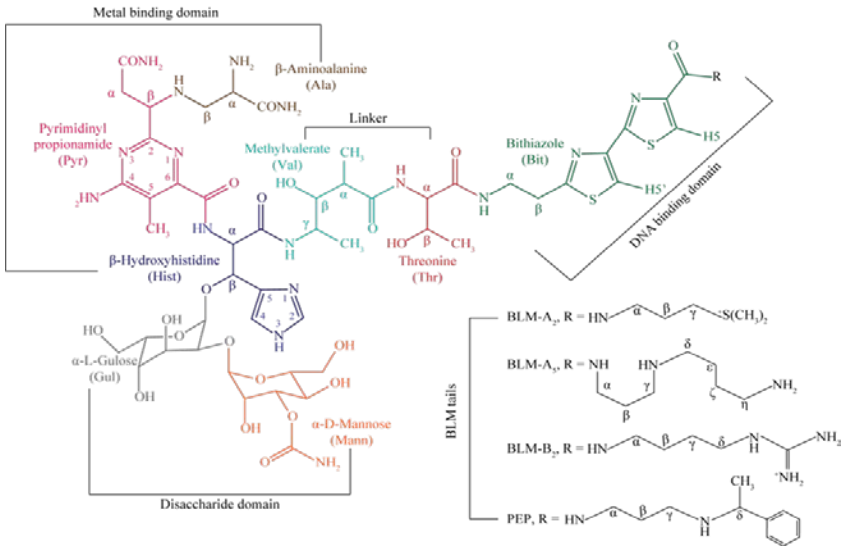

Figure 1: Structures of BLM-A_2, -B_2, -A_5, and peplomycin (PEP).

DNA Degradation: In its active form, BLM mediates a sequence selective, metal dependent oxidative cleavage of DNA [3]. The mechanism by which BLM induces a single- or double-

stranded break in DNA is dependent on the presence of O_2 and a redox-active metal, with Fe^{2+} being the cofactor proposed to act *in vivo*[32, 35, 51-53]. In aerobic conditions where Fe^{2+} is available for complexation, a BLM-iron-oxene and a C4' hydroperoxide undergo a Criegge-type rearrangement, which causes scission of the C3'-C4' deoxyribose bond and a single-stranded nick in the DNA [33, 48, 54]. For a double-stranded break to occur, the iron-oxene reacts with a C4' hydroperoxide on the opposite strand causing a similar scission event. The damage caused to the DNA initiates a degradation pathway, which in the case of cancer treatment is used to inhibit cancerous cell growth.

Toxicity: As mentioned previously, BLM treatment is sometimes associated with pulmonary fibrosis, a potentially fatal side effect that causes scarring in the lungs. Interestingly, different degrees of pulmonary fibrosis have been linked to the different structures of the BLM C-terminus [8-18]. According to biological studies performed by Raisfeld *et al*. [13-16], PEP and BLM-B_2 are less toxic in terms of pulmonary fibrosis than BLM-A_2 and -A_5. The clinically used form of the drug, Blenoxane, is a mixture of BLM-A_2 and -B_2 and has an intermediate toxicity. The therapeutic index of the different BLMs does not seem to be connected to their respective degree of toxicity, suggesting the potential for a version of the drug that could be a more effective antitumor agent and also less toxic. As it stands, the precise role of the C-terminus in instances of pulmonary damage is unclear; however, its involvement in DNA binding suggests the possibility of off-target effects where changes in the structures of the involved molecules could create undesired outcomes.

Experimental Design: Based on the above discussion on the different elements involved in the DNA-BLM interaction, we return to our research question: how do different BLMs and DNA

fragments affect the structure of the BLM-DNA complex upon binding, and can these structural relationships be connected to toxicity? To this end, we designed three separate investigations whereby we could isolate each variable and determine its effects on the structure using NMR spectroscopy. In our first study, we looked at the effect of Zn(II)BLMs (-A_2, -A_5, -B_2, and PEP) on the structure of a DNA hairpin (OL1: 5'-AGGCCTTTGGCCT-3'), which contained the 5'-GC-3' binding site. In our second study, we continued to look at the effect of Zn(II)BLMs (-A_2 and PEP) on the structure of a DNA hairpin (OL2: 5'-CCAGTATTTTTACTGG-3'), which contained the 5'-GT-3' binding site. Finally, in our third study, we looked at the effect of DNA hairpins OL1 and OL2, which contained the 5'-GC-3' and 5'-GT-3' binding sites, respectively, on the structure of Zn(II)BLMs (-A_2, -A_5, -B_2, and PEP). In this way, we determined the effects of the binding site and the BLM C-terminus on the structure of the drug and DNA fragment, respectively.

For these experiments, we selected Zn^{2+} as our metal center due to its diamagnetic character and inability to prompt DNA cleavage. We also designed DNA hairpins, where a short, self-complementary sequence folded upon itself to make a region of double-stranded DNA crowned by a loop. We found this to be a novel approach because the hairpin formation was considered energetically favorable when compared to another approach involving two complementary DNA strands. Based on preliminary studies, we were convinced that the hairpin method led to the formation of one double-stranded DNA sequence, as opposed to a mixture of products that was observed when we attempted to use two complementary DNA strands.

For the purpose of our studies, we used NMR spectroscopy to determine the different conformations of the drug and DNA strand of interest. Through two-dimensional nuclear Overhauser effect spectroscopy (NOESY) we were able to identify protons close to each other in space (within 5 Å apart). Likewise, through two-dimensional total correlation spectroscopy

(TOCSY) we could detect protons connected through a chain of coupling. The combination of these two spectra allowed us to represent the structures of the molecules in terms of the number of nuclear Overhauser effect cross signals (NOEs). Ultimately, we created cartoon depictions of the molecules where we represented each NOE connection as a line connecting two protons. The overall effect of these images was to create pictures of regions of the molecule that were being disturbed upon binding, based on which NOEs were conserved and which had disappeared relative to the original structure. Not only did the NOEs establish which protons were interacting with each other, but based on their unique chemical shift we could also deduce information about a proton's chemical and magnetic environment. A change in the chemical shift greater than 0.04 ppm was considered evidence of a proton being in a different chemical or magnetic environment upon binding, perhaps due to indirect contact with another molecule altering the original conditions. Ultimately, NMR provided us with the most detailed image of the DNA-BLM interactions, based on proton-proton connections and discrete changes in the local chemical and magnetic environments. In the end, the specificity of our data allowed us to create a very detailed and unadulterated image of the global effects related to BLM-DNA binding.

Sample Preparation and Data Collection: For each of the three investigations to be discussed, the sample preparation and data collection were the same. Samples of DNA were prepared at 0.5 mM concentrations with NaCl in D_2O and H_2O. Similarly, BLM samples were prepared at 3 mM concentrations with $ZnSO_4$ in D_2O and H_2O. The pH of both samples was adjusted to 6.5. TOCSY and NOESY spectra were collected for the DNA and drug separately at 5 and 25 °C.

The formation of the Zn(II)BLM:DNA complex was achieved by adding aliquots of Zn(II)BLM to DNA until a 1:1 molar ratio was reached. This process was followed using a one-

dimensional (1D) proton spectrum, which allowed us to monitor changes in regions involved with DNA binding. Upon addition of Zn(II)BLM to DNA, we observed broadening and shifting of signals in the aromatic protons of the BLM molecule and the imino protons of the DNA. Changes to these signals was indication of binding and stopped occurring once we reached a 1:1 Zn(II):BLM molar ratio. Using these samples, we again collected TOCSY and NOESY spectra at 5 and 25 °C in D_2O and H_2O.

NMR experiments were performed at 600 MHz on a Bruker AVANCE III 600 spectrometer. Corresponding spectra were processed and analyzed using Topspin 3.0 and NMRViewJ software.

Materials: BLM-A_2 and -B_2 sulfate were purchased from TOKU-E (Bellingham, WA). BLM-A_5 was purchased from LKT Laboratories, Inc. (St Paul, MN). PEP was a generous gift of Nippon Kayaku Co., Ltd. (Tokyo, Japan). Zinc sulfate 7-hydrate was purchased from VWR (Radnor, PA). Deuterated water (99.9%, d), sodium hydroxide, and sodium chloride were purchased from Sigma-Aldrich (St Louis, MO). The oligonucleotides were purchase from Integrated DNA Technologies, Inc. (Coralville, IA).

Investigation 1:

NMR Study of the Effects of Some Bleomycin C-termini on the structure of a DNA Hairpin with the 5'-GC-3' Binding Site

Teresa E. Lehmann, Sally A. Murray, Azure D. Ingersoll, Teresa M. Reilly, Shelby E. Follett, Kevin E. Macartney, Mark H. Harpster

Published: *J. Biol. Inorg. Chem*. 2016, *22*, 121-136.

The objective of this particular work was to study the effects of Zn(II)BLMs (-A_2, -A_5, -B_2, and PEP) on the conformation of a DNA hairpin containing a 5'-GC-3' binding site. The complete sequence of the DNA hairpin used was 5'-AGGCCTTTGGCCT-3' (OL1), which we validated through a round of preliminary NMR studies. Based on these initial experiments, which were the first I performed as an undergraduate researcher, we generated the following cartoon depictions of our unbound hairpin (free OL1) (Figure 2).

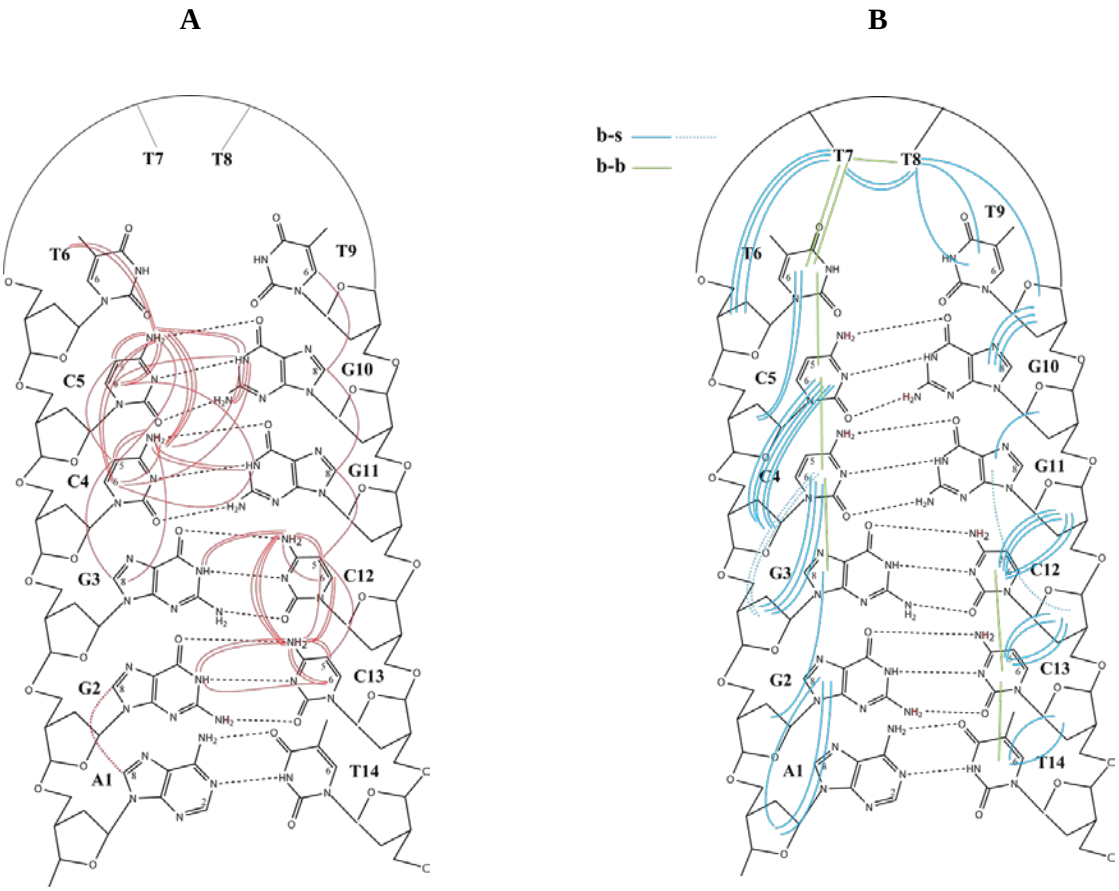

Figure 2: A) Schematic representation of free OL1 displaying amino and imino ^{1}H-^{1}H NOE connectivities (red) detected at 5 ºC in H_2O. B) Schematic representation of free OL1 displaying base-base (b-b, green) and base-sugar (b-s, blue) ^{1}H-^{1}H NOE connectivities detected at 25 ºC in D_2O. Dashed lines are used to avoid confusion in busy sectors of the figure.

After free OL1 was characterized through NMR, we produced Zn(II)BLM-bound OL1 by adding various aliquots of Zn(II)BLM to reach a 1:1 Zn(II)BLM:OL1 molar ratio. According to the procedure described above, we followed these additions by monitoring a 1D proton spectrum. As shown in Figures 3 and 4, peaks in the imino region of the DNA and aromatic region of BLM broaden and shift upon Zn(II)BLM addition. The change in these signals is evidence of Zn(II)BLM binding and stops occurring once a 1:1 molar ratio of the two molecules is reached. Upon closer examination, these peaks broaden and shift differently depending on which Zn(II)BLM is bound, suggesting a different binding conformation dependent on the BLM C-termini.

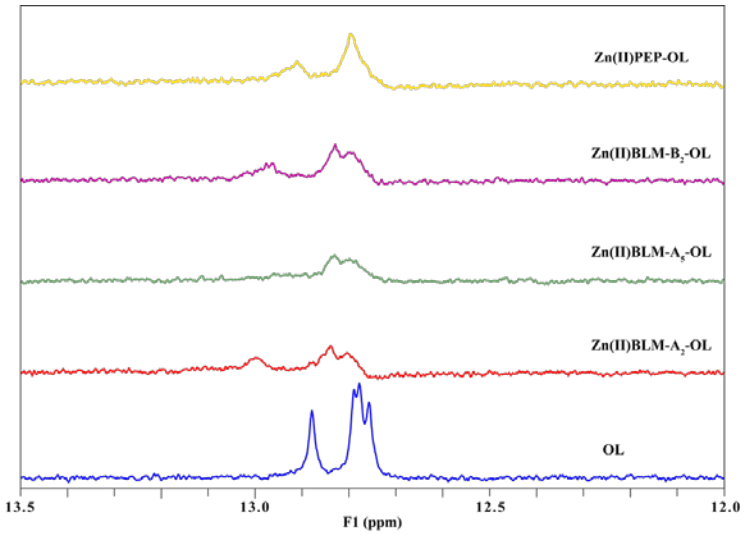

Figure 3: Imino region of the 1D ^{1}H-NMR spectra in H_2O collected at 5 ºC for free OL1 and OL1 bound to Zn(II)BLM-A_2, -A_5, -B_2, and Zn(II)PEP. Zn(II)BLM:DNA molar ratio 1:1.

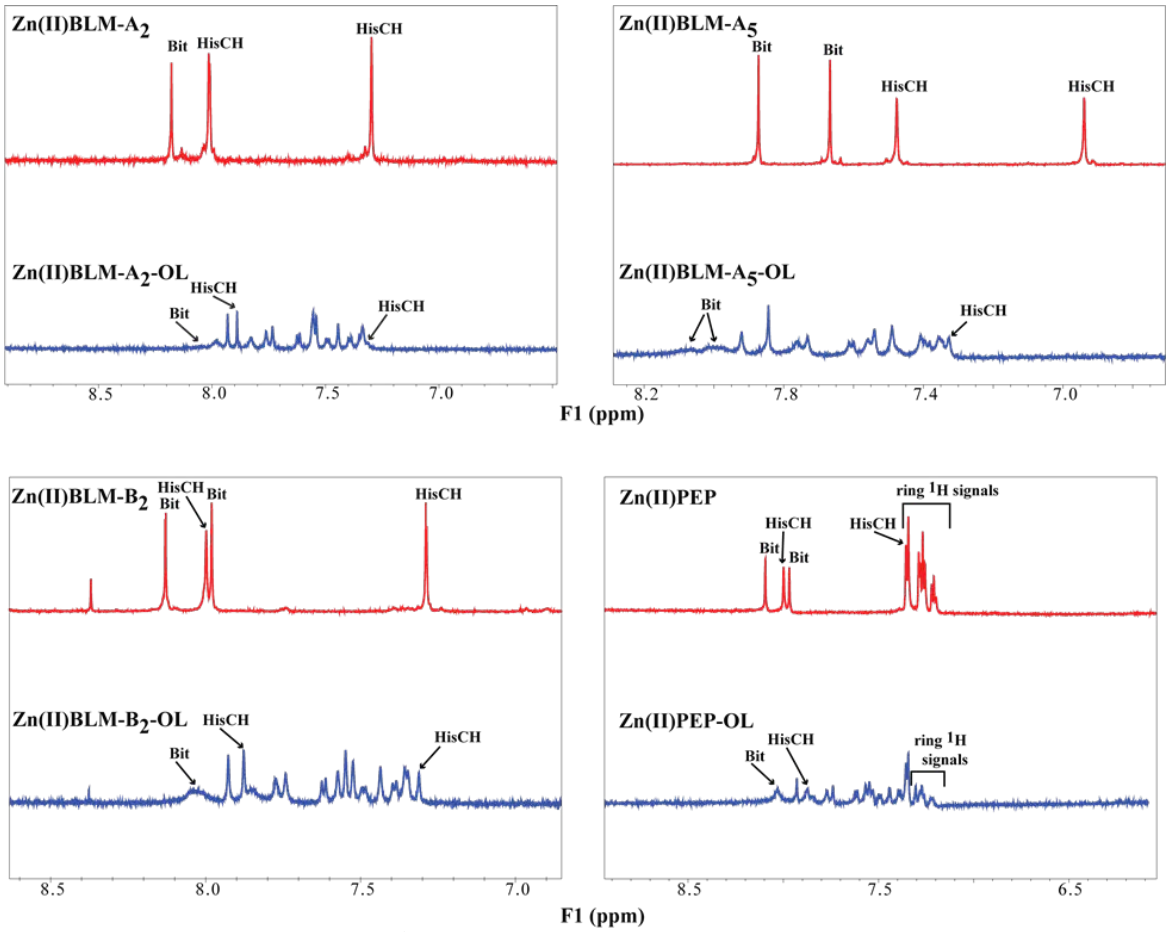

Figure 4: Aromatic region of the ^{1}H-NMR spectra collected at 25 ºC in D_2O of the free MBLMs and MBLMs bound to OL1. Zn(II)BLM:DNA molar ratio 1:1.

Upon addition of the Zn(II)BLMs to OL1, we collected TOCSY and NOESY spectra of the Zn(II)BLM-DNA complex (triad), which allowed us to compare the bound conformation of OL1 to its native conformation (free OL1). Based on changes in the number of free-OL1 NOEs observed in the spectra collected for the triads, we were able to measure how the native OL1 conformation was altered upon Zn(II)BLM binding. In the presence of Zn(II)BLM-A_2, -A_5, -B_2, and Zn(II)PEP, the percentage of conserved native NOEs in OL1 was 88%, 68%, 73%, and 71%, respectively. Interestingly, Zn(II)BLM-A_5 is the most toxic form of the drug, and causes the most disruption to OL1 (only 68% native NOEs conserved). These changes to the conformation of OL1 are to be visualized using the following schematic representations (Figures 5 and 6). Relative to

the native OL1 conformation (Figure 2), each OL1 molecule shows a disturbed conformation upon Zn(II)BLM binding. Furthermore, each Zn(II)BLM-bound OL1 molecule exhibits a different network of conserved native NOEs depending on which Zn(II)BLM is bound. In general, the internal conformation (inter-strand NOE connectivities) of OL1 is disrupted at the binding site (Figure 5), indicative of intercalation by the bithiazole moiety. The specific number of native NOEs present in the NOESY spectra collected for the triads in this region are different, for example Zn(II)PEP-OL1 has more native NOEs, indicating less disruption of the native conformation.

In regards to the core conformation of OL1 (base-base (b-b) and base-sugar (b-s) NOE connectivities), we observe that the number of native NOEs present in the right stand of OL1 has decreased in the triads (Figure 6). This trend could be related to the mode of binding of Zn(II)BLM to OL1. We conjecture that the BLM tail interacts with the right strand of OL1 after bithiazole intercalation, modifying its original conformation. Additionally, new NOEs observed in the triads are concentrated on the left side of the strand, which could be an effect of the tail interacting on the right and forcing new connections.

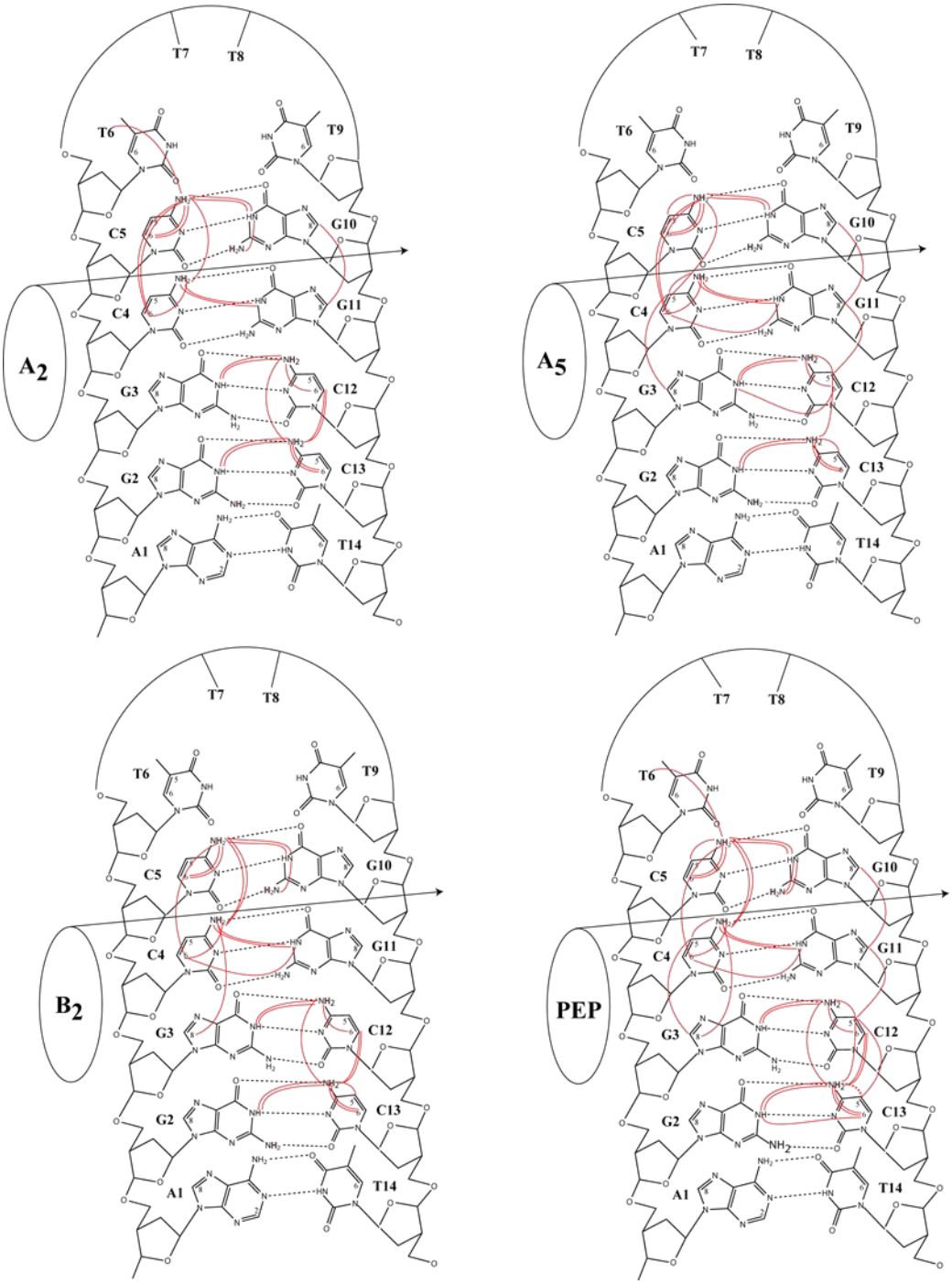

Figure 5: Schematic representation of OL1 bound to Zn(II)BLMs displaying the ^{1}H-^{1}H inter-strand NOE connectivities detected at 5 ºC in H_2O.

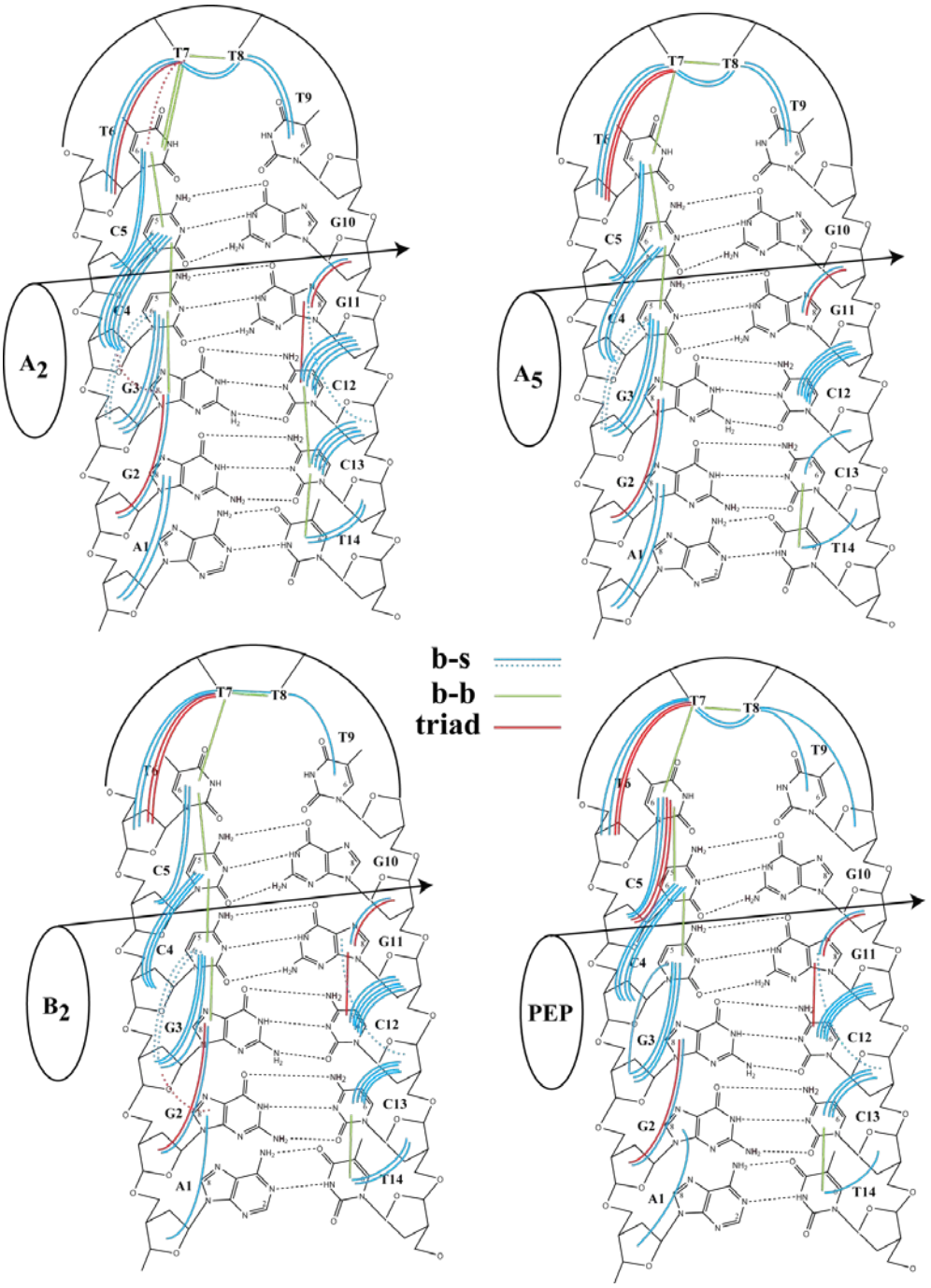

Figure 6: Schematic representation of OL1 bound to MBLMs displaying the core ^{1}H-^{1}H NOE connectivities detected at 25 ºC in D_2O. Base-base (b-b, green), base sugar (b-s, blue), and NOEs only found upon Zn(II)BLM binding (red).

Another dimension of this study allowed us to determine which protons experienced a significant change in chemical shift (Δδ) upon binding to Zn(II)BLM. We represented these

changes in Figure 7, where highlighted bases exhibited Δδs greater than or equal to 0.04 ppm. Consistent amongst the four structures, the bases around the binding site are all significantly affected. However, depending on which BLM is bound, we observe different changes in the chemical shifts throughout the molecule. For example, Zn(II)BLM-A_5 has the most bases affected, especially in the loop and at the termini, which suggests a more widespread effect of the drug upon binding.

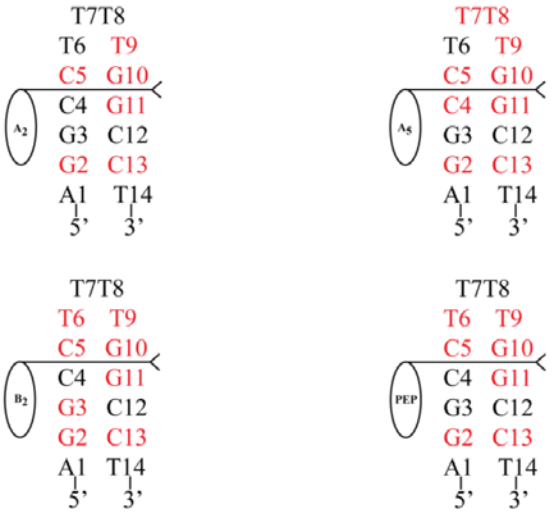

Figure 7: Schematic representation of OL1 bound to Zn(II)BLMs indicating the DNA bases exhibiting significant changes in chemical shifts ($\Delta\delta$ greater than or equal to 0.04 ppm) upon Zn(II)BLM complexation in *red.*

The results of this study confirm that, in the context of the 5'-GC-3' DNA-binding site, the C-termini of the drug has a direct effect on how the conformation of OL1 changes, as determined by chemical shift differences and number of native and new NOE connectivities detected in the triads. Despite there not being a clear relationship between the C-termini and pulmonary toxicity, we find that the more toxic the BLM, the more the OL1 structure is disturbed upon binding, as is the case when Zn(II)BLM-A_5 is bound to OL1.

Investigation 2:

Interaction of Zn(II)Bleomycin-A_2 and Zn(II)peplomycin with a DNA Hairpin containing the 5'-GT-3' Binding Site in Comparison with the 5'-GC-3' Binding Site Studied by NMR Spectroscopy

Shelby E. Follett, Azure D. Ingersoll, Sally A. Murray, Teresa M. Reilly, Teresa E. Lehmann*

Published: *J. Biol. Inorg. Chem.* 2017, 22, 1039-1054

We continued our investigation on the structural relationship between the BLM C-termini and the DNA-binding site by expanding our research to include a DNA hairpin containing the 5'-GT-3' binding site. In this particular work we look at the effect of Zn(II)BLM-A_2 and Zn(II)PEP on the structure of a DNA hairpin of sequence 5'-CCAGTATTTTTACTGG-3' (OL2), which we validated through a round of preliminary NMR studies. To the NMR samples of - OL2, we added various aliquots of Zn(II)BLM-A2 and Zn(II)PEP. As in our previous study, we followed this addition by monitoring 1D ^{1}H-NMR spectra. Again, we observed broadening and shifting of the imino signals of OL2 in the triads, indicating Zn(II)BLM binding.

Reminiscent of Investigation 1, we created similar cartoon depictions of OL2 before and after Zn(II)BLM binding (Figures 8, 9, and 10). As in Investigation I, Figures 9 and 10 indicate that binding of Zn(II)BLM-A_2 and Zn(II)PEP produce changes in the native-NOE network in OL2, reinforcing the notion that the BLM tail has an influence on the conformation of the OL. Regarding the native-OL2 NOEs that are conserved after Zn(II)BLM complexation, Figure 9 shows that most of the connections in the region above the binding site are lost, indicating that the BLM is disrupting the interior of the hairpin above the binding site to a greater extent than below the binding site. Overall, out of 62 inter-strand native NOEs detected for free OL2, the PEP triad conserves 31% and the A_2 triad conserves 35% of the exchangeable protons. This is a significant

difference compared to the Zn(II)PEP-OL1 complex, which conserved 64% of the free-OL1 NOEs in this region, and the Zn(II)BLM-A_2-OL1 complex, which conserved 43% of these NOEs. The conserved NOEs for OL1 are equally distributed along the interior of the hairpin (Investigation I), whereas these NOEs for OL2 are concentrated below the binding site. These results are an indication that the inter-strand native structure of OL2 is, in general, disrupted to a greater extent than that of OL1 as a consequence of Zn(II)BLM binding. Additionally, the 5'-GT-3' binding site seems to undergo significant restructuring in the presence of the drugs, as indicted by the loss of the NOEs between the base pairs A6NH_2-T11NH and A12NH_2-T5NH protons.

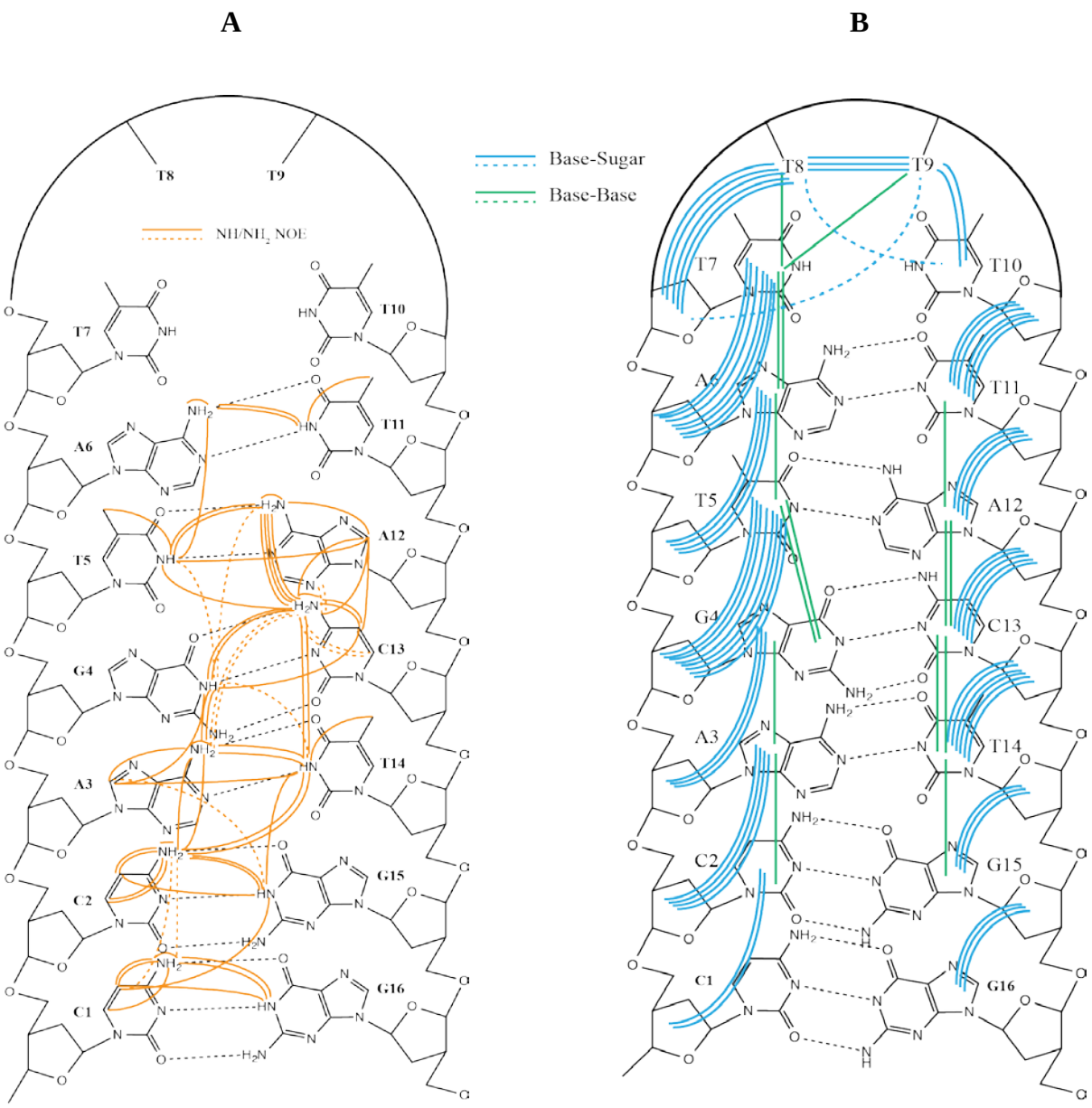

Figure 8: A) Schematic representation of the NOE connections between the exchangeable protons in free OL2 in H_2O at 5 °C. B) Schematic representation of the NOE connections for free OL_2 in D_2O at 25 °C. Base-base (green) and base-sugar (blue) NOEs . Dashed and continuous lines both represent NOEs, and are used together to avoid confusion in busy regions of the scheme.

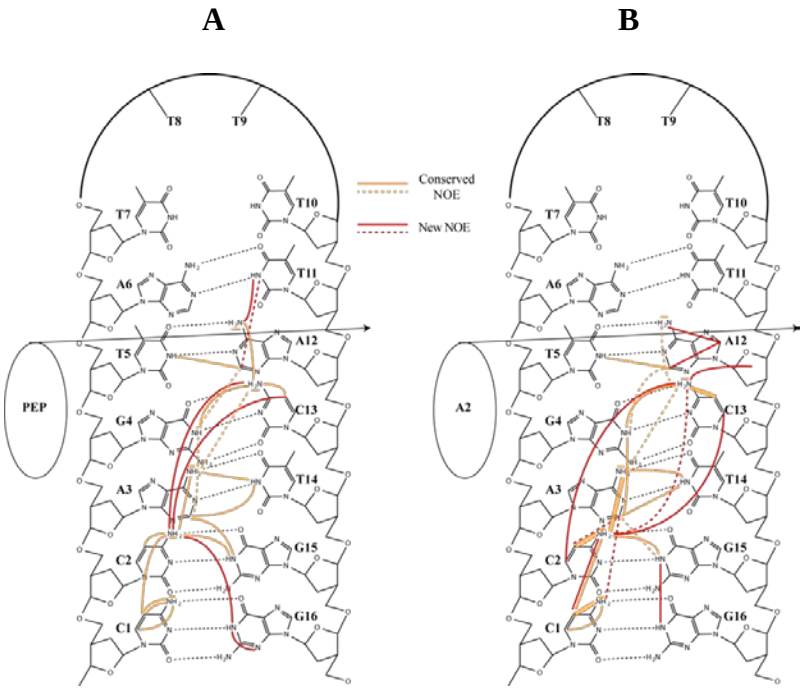

Figure 9 : Schematic representation of the NOEs between the exchangeable protons for OL2 bound to Zn(II)BLMPEP (A) and Zn(II)BLM-A2 (B) in H_2O at 5 °C, showing the native (orange) and new (red) NOEs detected in the triads. Dashed and continuous lines both represent NOEs, and are used together to avoid confusion in busy regions of the scheme.

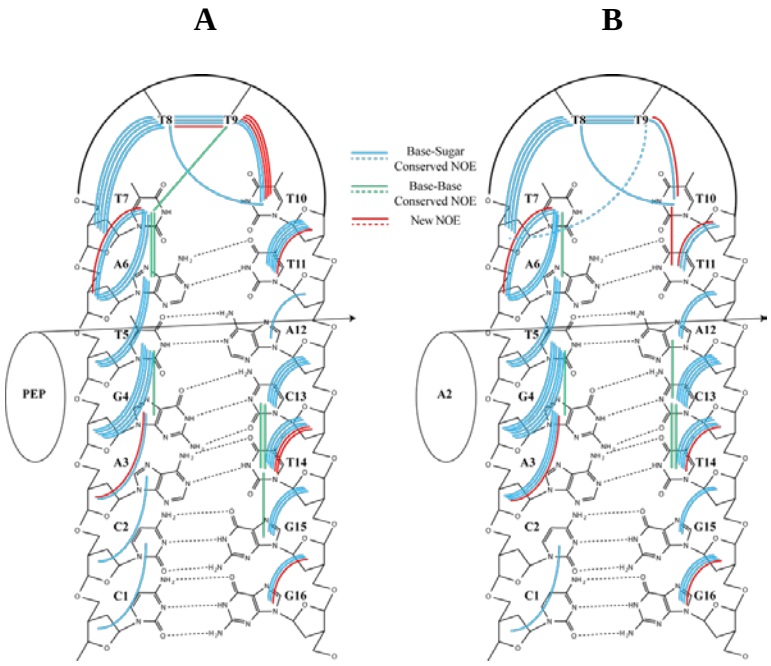

Figure 10: Schematic representation of the core NOE connections for OL_2 bound to Zn(II)PEP (A) and Zn(II)BLM-A2 (B) in D_2O at 25 °C, showing the native base-base (green), native base-sugar (blue), and new (red) NOEs detected in the triads. Dashed lines are used to avoid confusion in the busy sectors of the scheme.

Interestingly, for both complexes we also observe a number of intermolecular NOEs that connect the hairpin directly to the drug (Figure 11). This type of NOE was not detected in the previous investigation involving the 5'-GC-3' binding site, and suggests that OL2 and the Zn(II)BLMs examined herein are closer in space than in the OL1 triads.

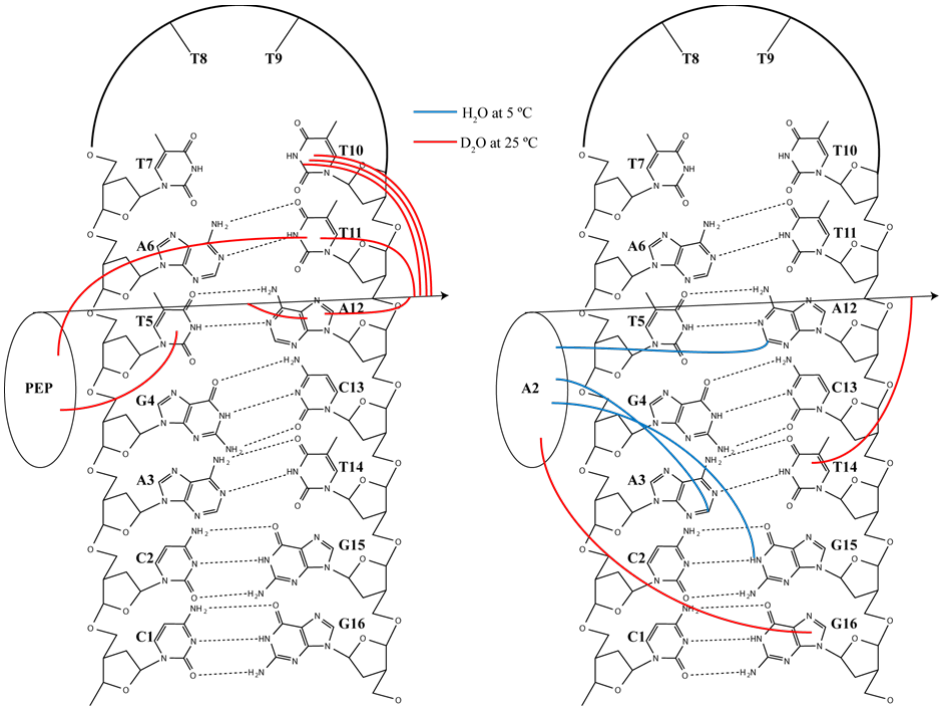

Figure 11: Schematic repentation of the intermolecular NOEs detected after MBLM complexation.. Blue and red lines represent NOEs detected in H_2O at 5 °C and D_2O at 25 °C, respectively.

It is worth noticing that these NOEs differ in number and in the connected protons between the two triads, indicating that the BLM C-terminus has an effect on the interaction between drug and target.

In order to further study the different binding relationships, we determined the Zn(II)BLM:DNA dissociation constant for each triad. We performed an equilibrium dialysis procedure whereby the DNA could non-competitively bind to the Zn(II)BLM based on its affinity

for the drug. For Zn(II)BLM-A_2 bound to OL1 and OL2, the experimental dissociation constants were found to be 4.3×10^{-6} and 3.1×10^{-6} M, respectively. Likewise, for Zn(II)PEP bound to OL1 and OL2, the experimental dissociation constants were found to be 1.5×10^{-5} and 6.7×10^{-6} M, respectively. The smaller dissociation constants observed for both Zn(II)BLMs bound to the OL2 suggests overall tighter binding at the 5'-GT-3' binding site.

Again we compared the bases that experienced significant changes in their chemical shift upon binding (Figure 12). Looking at Zn(II)BLM-A_2 and Zn(II)PEP bound to OL2, we observe a different pattern of bases affected for each complex. When these same Zn(II)BLMs were bound to OL1, we observe less bases affected upon binding. The increased number of affected bases in OL2 suggest more disruption to the DNA structure upon binding. This is most likely explained by a more involved interaction between the two molecules in the OL2 triads, which is simplified when the same Zn(II)BLMs bind to OL1.

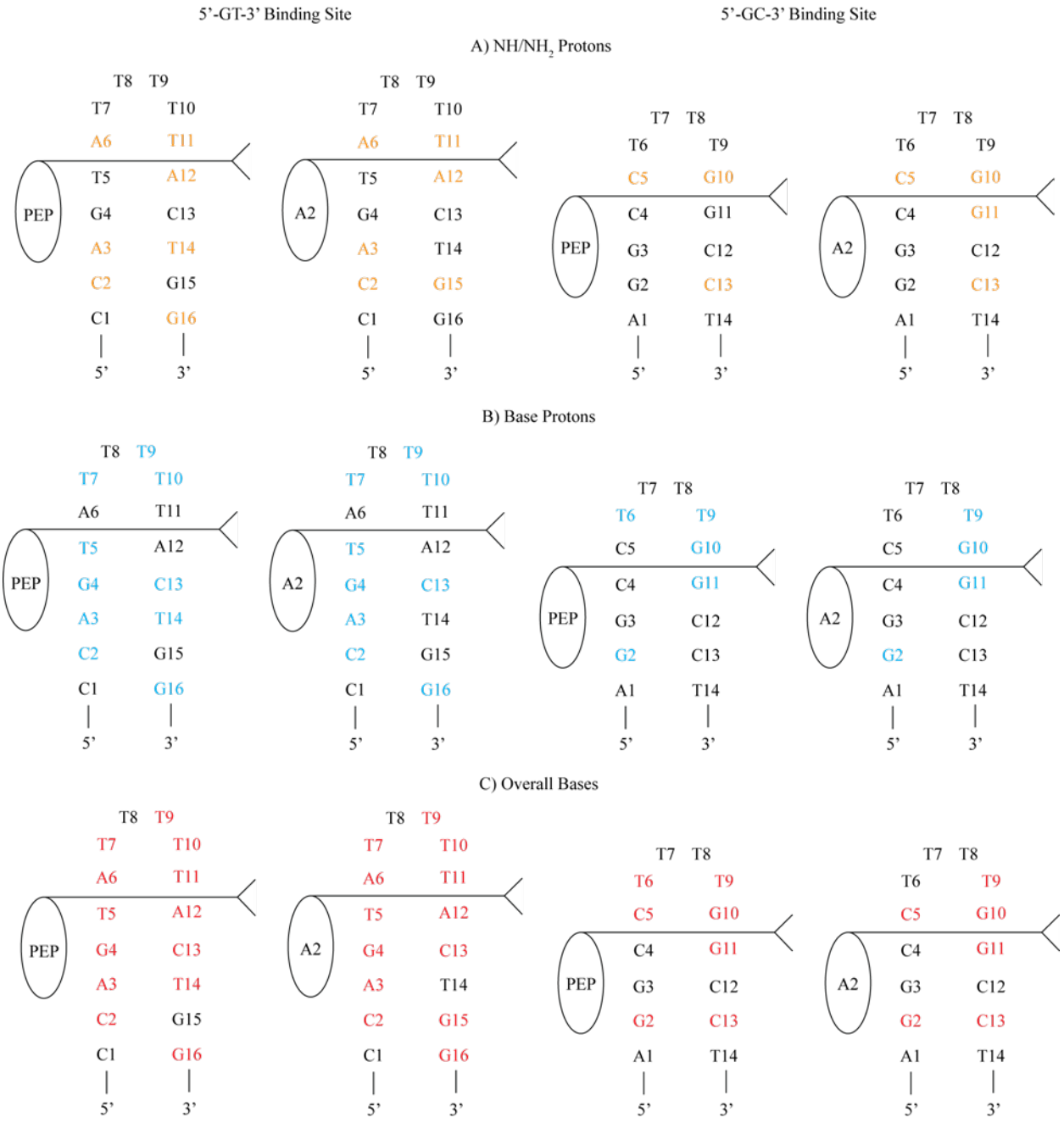

Figure 12: Schematic comparison of the effects that Zn(II)BLM-A_2 and Zn(II)PEP have on OL2 and OL1. Colored DNA bases experince $\Delta\delta$ greater than or equal to |0.04| ppm upon Zn(II)BLM complexation for: (A) Imino/amino protons (orange), (B) base protons (blue), (C) and an overall comparison (red) are presented.

Ultimately, the results of this study show that Zn(II)BLM-A2 and Zn(II)PEP affect the structure of OL2 differently upon complexation. Another dimension of this study shows that these

changes also depend on the binding site in the oligonucleotides studied. Our results show that the Zn(II)BLMs bind tighter to the 5'-GT-3' binding site than the 5'-GC-3' binding site, which may explain why we observe more dramatic structural effects in the complexes involving the OL2. In this way, a tighter binding could correspond to improved cleavage efficiency in DNA segments containing abundant 5'-GT-3' binding spots.

Investigation 3:

Structural changes of multiple analogs of bleomycin when bound to DNA hairpins containing the 5'-GT-3' binding site and 5'-GC-3' binding site studied by NMR spectroscopy

Shelby E. Follett, Sally A. Murray, Azure D. Ingersoll, Teresa M. Reilly, Teresa E. Lehmann*

Accepted for pulication in the NMR Special Issue of *J. Magnetochemistry*

In our third and final study we look at the effect of OL1 and OL2 on the conformation of Zn(II)BLM-A_2, -A_5, -B_2, and Zn(II)PEP. Similar to the previous two studies, we look at changes in chemical shift and conserved native NOEs in the OL1 and OL2 triads, but this time in the context of the Zn(II)BLM structure. Shown below are the native intramolecular NOEs observed for each Zn(II)BLM structure (Figure 13).

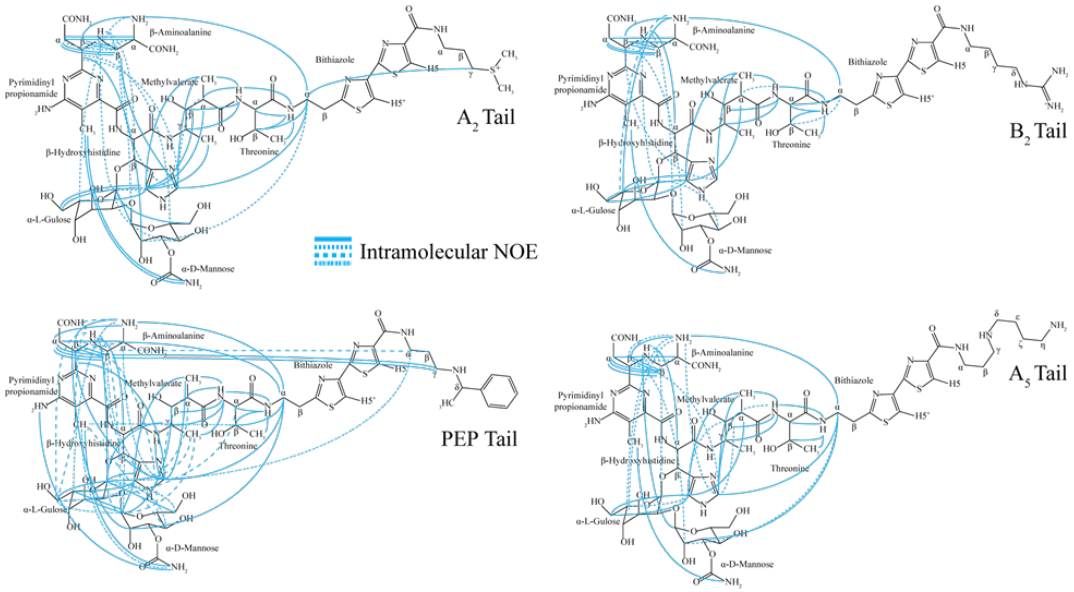

Figure 13: Inter-residue intramolecular NOE connectivities for each Zn(II)BLM under study before binding to OL1 and OL2 for spectra acquired in H_2O at 5 °C.

Upon complexation to OL1, we observe a different pattern of intramolecular NOEs for each drug relative to its unbound form (Figure 14). Furthermore, when Zn(II)BLM-A_2 and Zn(II)PEP form complexes with OL2, we observe differences in each structure that are also dissimilar to the OL1 complexes (Figure 15). For example, Zn(II)PEP has a lot of NOE connectivities when it is bound to OL1; however, its intramolecular connections are very sparse when the drug is bound to OL2. This could be related to the binding affinity discussed earlier, and how tighter binding at the 5'-GT-3' site could disturb the structure to a greater degree. Ultimately, the different Zn(II)BLM structures suggest rearrangement of the Zn(II)BLM after complexation, and could relate to different degrees of cleavage efficiency allowed by the binding formation.

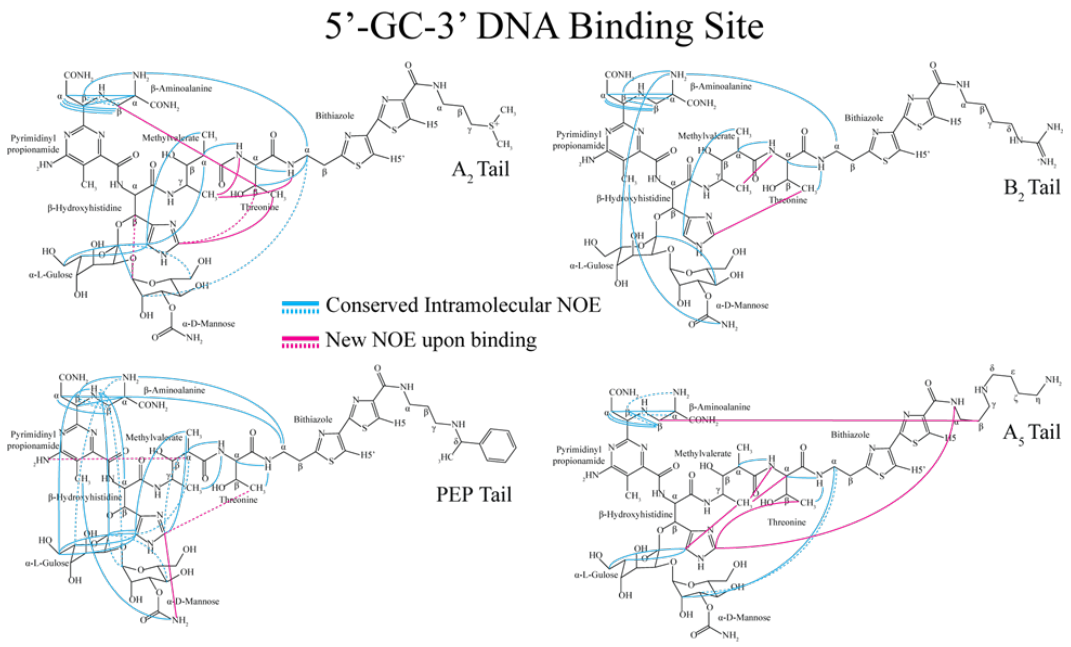

Figure 14: Inter-residue intramolecular NOE connectivities for each Zn(II)BLM under study after binding to OL1. Samples of Zn(II)BLM:OL1 are in a 1:1 molar ratio in H_2O at 5 °C.

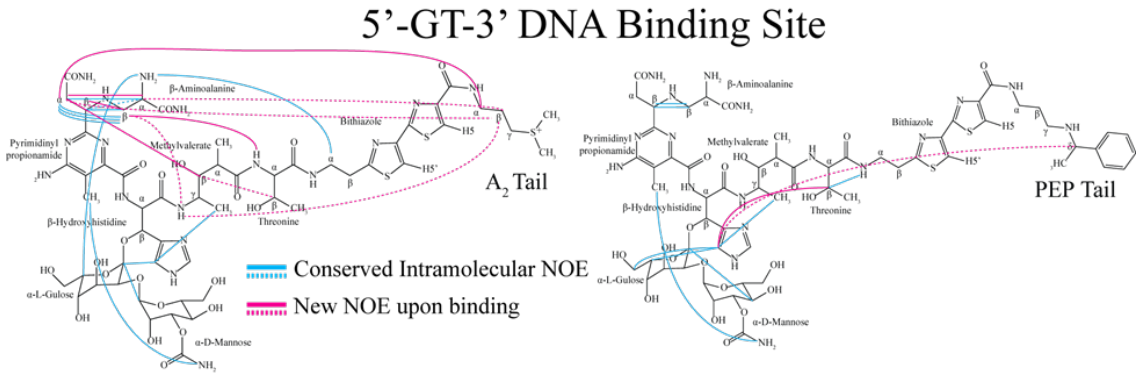

Figure 15: Inter-residue intramolecular NOE connectivities for each Zn(II)BLM under study bound to OL2. Samples of Zn(II)BLM:OL2 are in a 1:1 molar ratio in H_2O at 5 °C.

For the Zn(II)BLM structures studied, we also determined which protons experienced a significant change in their chemical shift upon binding. Again for different combinations of Zn(II)BLM and OL, we observed a different pattern of protons affected by binding (Figures 16 and 17). Note that in all cases the metal binding domain and linker domain are concentrated regions where protons are significantly shifted. This suggests that there are different chemical and

magnetic environments for the metal coordination cage, depending on the C-termini and the OL bound. Similarly, dramatic changes in the linker region could also affect its structure such as to make DNA cleavage more or less efficient.

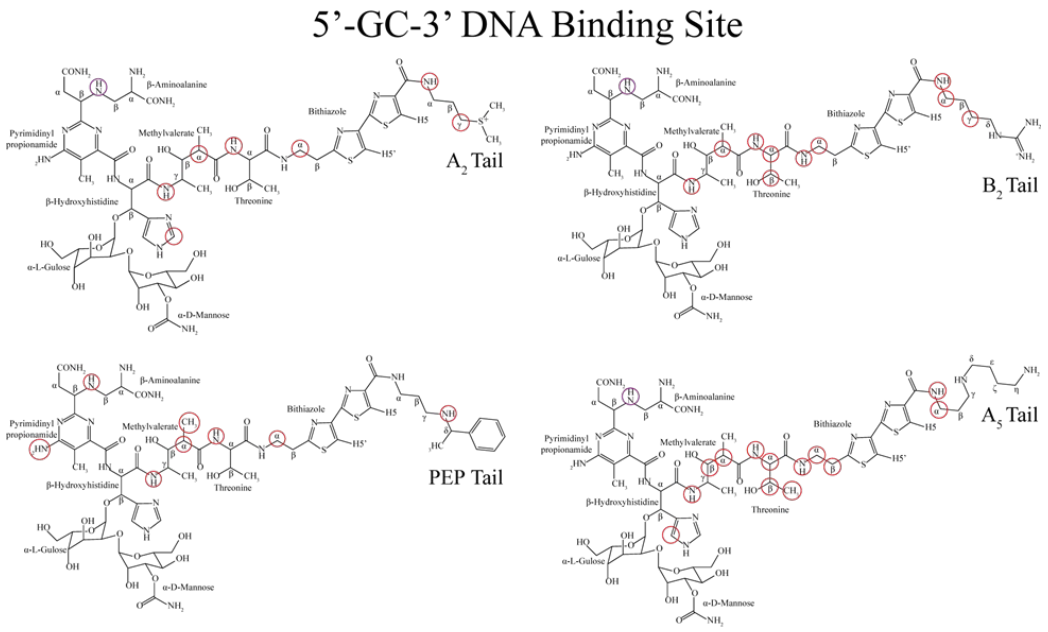

Figure 16: Zn(II)BLM protons signals that significantly shift (red circles) or no longer can be assigned (purple circles) upon binding to OL1 in a Zn(II)BLM:OL1 1:1 molar ratio for spectra acquired in H_2O at 5 °C.

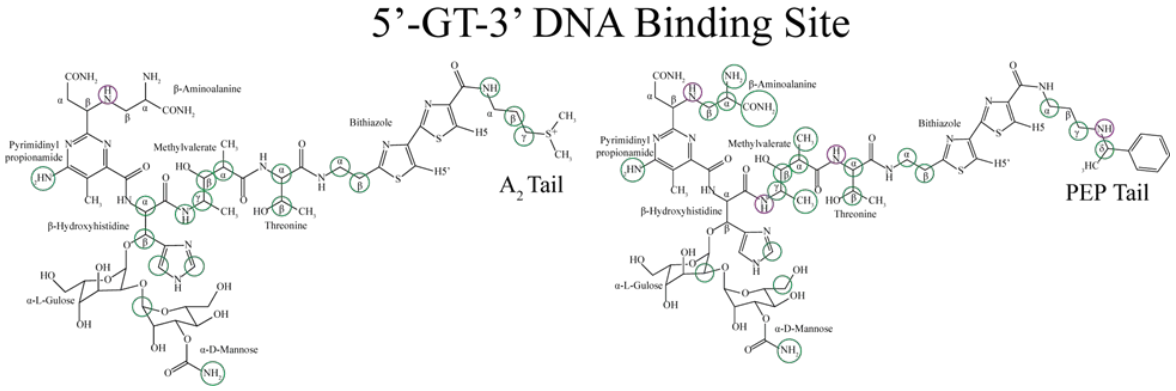

Figure 16: Zn(II)BLM protons signals that significantly shift (green circles) or no longer can be assigned (purple circles) upon binding to OL2 in a Zn(II)BLM:OL2 1:1 molar ratio for spectra acquired in H_2O at 5 °C.

In conclusion, our third study showed that the conformation of each Zn(II)BLM is different depending on its C-terminus and the binding site used. It is possible, but not confirmed, that the different conformations allowed by the binding interactions could lead to more efficient DNA cleavage, which could be related to the therapeutic index and toxicity for the drug.

General Conclusions: The significant findings of our research include showing that of the two preferential binding sites (5'-GC-3' and 5'-GT-3'), one is more preferred (5'-GT-3'). Another important contribution was showing that the BLM C-terminus does play a role in determining the conformation of the DNA segment upon binding. These results provide consistency and comparability within our field, which it had been previously lacking. We hope that elucidating the complicated interaction between BLM and DNA will help in the design of a more efficient and less toxic BLM analog.

In the future, we would like to study the biologically active complex, Fe(II)BLM and see if the trends we observed here hold true. Studying Fe(II)BLM presents various challenges, including that Fe(II) is paramagnetic and therefore hard to analyze with NMR. Additionally, samples will have to prepared anaerobically in order to ensure that DNA is not cleaved.

We have also looked into studying the effects of BLM on RNA. Fe(II)BLM has been reported as mediating degradation of certain RNA substances. Interestingly, there are deposits of RNA molecules throughout the lungs which could be the target of BLM in the case of pulmonary damage.

Reflections: The final paper I wrote in freshman colloquium was a sort of manifesto in defense of "not knowing" specifically, not knowing what I wanted to be when I grew up. I managed to relate

this concept of “not knowing” to all the texts we had read, and arrive at the somewhat cliché conclusion that in light of being uncertain, I could be more receptive to the meaning behind each moment. As a fifth year senior, rereading my paper is a little embarrassing. It has the angsty tone that only a fresh high school graduate can pull off. It is also transparent to me now that I wanted to “find myself,” probably like how Elizabeth Gilbert found herself in “Eat, Pray, Love”. I even went to Italy, but that is a different story. Now, as I write my honors thesis, I have the advantage of perspective and knowing that I did eventually realize what I wanted to be when I grew up – a researcher. No doubt, certain innate qualities about myself have led me to these crossroads, where I am graduating college as a double major in chemistry and molecular biology and pursuing further education. However, in regards to defining moments, no single, isolated event stands out to me more than when I joined the Lehmann Group.

In the spring semester of my sophomore year, I replied on a whim to a campus-wide email regarding a research opportunity in the chemistry department. Almost as random as my interest was the fact that I was one of two undergraduate students selected for the position, thus marking the beginning of my work with Dr. Teresa Lehmann. At the point when I was hired, I was still uncertain about mostly everything, but after working for Dr. Lehmann for six months, I declared a second major in chemistry in addition to what I was already pursuing in molecular biology. I became obsessed with trying to visualize interactions on the atomic and molecular scale and relating those to observed changes in an organism or larger system. I gained access to a different part of my conscious that was motivated to make positive, lasting change by understanding complicated biochemical systems. Participating in meaningful research became my passion, as if all along I had wanted to grow up and be a scientist. In the end, and this is by no means the final end, I learned the importance of taking advantage of opportunity and working hard. This

experience has provided me with everything I need to move forward, which hopefully includes pursuing a Ph.D. in chemistry or biochemistry at the University of Washington. For the past four years, it has been refreshing for me to feel like I've been at the right place, at the right time, and I am excited to move on from here knowing that feeling and trusting that I will be able to recognize when I find it again.

Acknowledgements: Working on this project and reflecting on the past four years, I realize that I owe so much to Dr. Lehmann for guiding me through this seminal time and helping me become a better scientist and woman in science, specifically. I'm exceedingly proud of everything I've learned and everything that we've accomplished together. Words cannot express my gratitude for the time she has invested in my education and personal development. I hope she knows what a difference she makes and how much I've enjoyed working for her. She will forever be one of my most cherished role models. To everyone else who has been a part of the Lehmann Group, Azure and Terry – thank you for being wonderful friends and coworkers throughout the years.

I would also like to thank the Honors College for being dedicated to providing a truly comprehensive education that transcends the traditional curriculum. As part of the program, I benefited from taking a wide range of classes that exposed me literature and art, as well as issues involving social justice and global awareness. The faculty within the program is tremendously supportive and encourages creativity and acceptance. Some of the most meaningful lessons I learned in college were initiated by different lectures and topics I was introduced to in my honors classes.

I would also like to thank UW and greater Laramie community for all they do to make our university a happy and safe learning environment.

Lastly, I would like to thank my family and friends for their continuous support and constant inspiration.

References:

1. Umezawa, H., Maeda, K., Takeuchi, T. & Okami, Y. New antibiotics bleomycin A and B. *J. Antibiot.* 19, 200-209 (1966).
2. Takita, T., Muraoka, Y., Nakatani, T., Fujii, A., Umezawa, Y., Naganawa, H., & Umezawa, H. Chemistry of bleomycin. 19. Revised structures of bleomycin and phleomycin. *J. Antibiot.* 31, 801-804 (1978).
3. Umezawa, H. in *Bleomycin: chemical, biochemical and biological aspects*. 24-36 (Springer, 1997).
4. Bennett, J. M. & Reich, S. D. Bleomycin. *Ann. Intern. Med.* 90, 945-948 (1979).
5. Hecht, S. M. in *Cancer Chemotherapeutic Agents*. 369-388 (ACS Professional Reference Book, 1995).
6. Einhorn, L. H. & Donohue, J. Cis-Diamminedichloroplatinum, vinblastine, and bleomycin combination chemotherapy in disseminated testicular cancer. *Ann. Intern. Med.* 87, 293-298 (1977).
7. Carlson, R. W., Sikic, B. I., Turbow, M. M. & Ballon, S. C. Combination cisplatin, vinblastine, and bleomycin chemotherapy (PVB) for malignant germ-cell tumors of the ovary. *J. Clin. Oncol.* 1, 645-651 (1983).
8. Raisfeld, I. H., Chovan, J. P. & Frost, S. Bleomycin pulmonary toxicity: production of fibrosis by bithiazole-terminal amine and terminal amine moieties of bleomycin. A2. *Life Sci.* 30, 1391-1398 (1982).
9. Raisfeld, I. H., Chu, P., Hart, N. K., Lane, A. A comparison of the pulmonary toxicity produced by metal-free and copper-complexed analogs of bleomycin and phleomycin. *Toxicol. Appl. Pharm.* 63,351-362 (1982).
10. Raisfeld, I. H. Pulmonary toxicity of bleomycin analogs. *Toxicol. Appl. Pharm.* 56, 326-336 (1980).
11. Tanaka, W. & Takita, T. Pepleomycin - 2nd generation bleomycin chemically derived from bleomycin A2. *Heterocycles* 13, 469-476 (1979).
12. Oka, S. A review of clinical studies of pepleomycin. *Recent Results Cancer Res.* 74, 163-171 (1980).
13. Raisfeld, I. H., Kundahl, E. R., Sawey, M. J., Chovan, J. P. & Depasquale, J. Selective toxicity of specific lung-cells to bleomycin. *Clin. Res.* 30, A437 (1982).
14. Raisfeld, I. H. Relation between bleomycin structure and pulmonary fibrosis. *Clin. Pharmacol. Ther.* 29, 274 (1981).
15. Raisfeld, I. H. Relation of bleomycin structure to pulmonary toxicity. *Clin. Res.* 28, A530 (1980).
16. Raisfeld, I. H. Bleomycin terminal groups produce pulmonary fibrosis. *Clin. Res.* 27, A445 (1979).
17. Takahashi, K., Aoyagi, H. S., Koyu, A., Kuramochi, H., Yoshioka, O., Matsuda, A., Fujii, A., & Umezawa, H. Biological studies on the degradation products of 3-(S)-1'-phenylethylamino propylaminobleomycin-A novel analog (Pepleomycin). *J. Antibiot.* 32, 36-42 (1979).

18. Ito, K., Handa, J., Irie, Y., Ezura, H., Kumagai, M., Irie, Y., Suzuki, A., Hagiwara, T., Yamane, H., Miyamoto, K., Yamashita, T., Tsubosaki, M., Matsuda, A. N., & Konoha, N. Toxicological studies on pepleomycin sulfate (NK631). VI. Chronic toxicity of pepleomycin in dogs. *J. Antibiot.* 32, 387-450 (1979).
19. Caceres-Cortes, J., Sugiyama, H., Ikudome, K., Saito, I., & Wang, A. H. J. Interactions of deglycosylated Cobalt(III)-pepleomycin (green form) with DNA based on NMR structural studies. *Biochemistry* 36, 9995-10005 (1997).
20. Hoehn, S. T., Junker, H. D., Bunt, R. C., Turner, C. J. & Stubbe, J. Solution structure of Co(III)-bleomycin-OOH bound to a phosphoglycolate lesion containing oligonucleotide: Implications for bleomycin-induced double-strand DNA cleavage. *Biochemistry* 40, 5894-5905 (2001).
21. Lui, S. M., Vanderwall, D. E., Wu, W., Tang, X. J., Turner, C. J., Kozarich, J. W., & Stubbe, J. Structural characterization of Co center dot bleomycin A2 brown: Free and bound to d(CCAGGCCTGG). *J. Am. Chem. Soc.* 119, 9603-9613 (1997).
22. Manderville, R. A., Ellena, J. F. & Hecht, S. M. Interaction of Zn(II)-bleomycin with D(CGCTAGCG)(2). A binding model based on NMR experiments and restrained molecular dynamics calculations. *J. Am. Chem. Soc.* 117, 7891-7903 (1995).
23. Vanderwall, D. E., Lui, S. M., Wu, W., Turner, C. J., Kozarich, J. W., & Stubbe, J. A model of the structure of HOO-Co bleomycin bound to d(CCAGTACTGG): Recognition at the d(GpT) site and implications for double-stranded DNA cleavage. *Chem. Biol.* 4, 373-387 (1997).
24. Wu, W., Vanderwall, D. E., Stubbe, J. A., Kozarich, J. W. & Turner, C. J. Interaction of CO-bleomycin A2 (Green) with d(CCAGGCCTGG)(2): Evidence for intercalation using 2D NMR. *J. Am. Chem. Soc.* 116, 10843-10844 (1994).
25. Wu, W., Vanderwall, D. E., Lui, S. M., Tang, X. J., Turner, C. J., Kozarich, J. W., & Stubbe, J. Studies of Co Bleomycin A2 green: Its detailed structural characterization by NMR and molecular modeling and its sequence-specific interaction with DNA oligonucleotides. *J. Am. Chem. Soc.* 118, 1268-1280 (1996).
26. Wu, W., Vanderwall, D. E., Turner, C. J., Kozarich, J. W. & Stubbe, J. Solution structure of Co Bleomycin A2 green complexed with d(CCAGGCCTGG). *J. Am. Chem. Soc.* 118, 1281-1294 (1996).
27. Wu, W., Vanderwall, D. E. , Teramoto, S., Lui, S. M., Hoehn, S. T., Tang, X. J., Turner, C. J., Boger, D. L., Kozarich, J. W., & Stubbe, J. NMR studies of Co deglycoBleomycin A2 green and its complex with d(CCAGGCCTGG). *J. Am. Chem. Soc.* 120, 2239-2250 (1998).
28. Wu, W., Vanderwall, D. E., Turner, C. J., Hoehn, S., Chen, J. Y., Kozarich, J. W., & Stubbe, J. Solution structure of the hydroperoxide of Co(III) phleomycin complexed with d(CCAGGCCTGG)(2): evidence for binding by partial intercalation. *Nucleic Acids Res.* 30, 4881-4891 (2002).
29. Zhao, C. Q. *et al.* Structures of HO2-Co(III)bleomycin A2 bound to d(GAGCTC)(2) and d(GGAAGCTTCC)(2): structure-reactivity relationships of Co and Fe bleomycins. *J. Inorg. Biochem.* 91, 259-268 (2002).
30. Goodwin, K. D., Lewis, M. A., Long, E. C. & Georgiadis, M. M. Crystal structure of DNA-bound Co(III)-bleomycin B-2: Insights on intercalation and minor groove binding. *Proc. Natl. Acad. Sci. USA* 105, 5052-5056 (2008).

31. Kane, S. A. & Hecht, S. M. in *Progress in Nucleic Acid Research and Molecular Biology* Vol. 49 (eds E. Cohn Waldo & Moldave Kivie) 313-352 (Academic Press, 1994).
32. Hecht, S. M. The chemistry of activated bleomycin. *Accounts Chem. Res.* 19, 383-391 (1986).
33. Stubbe, J. & Kozarich, J. W. Mechanisms of bleomycin-induced DNA-degradation. *Chem. Rev.* 87, 1107-1136 (1987).
34. Sausville, E. A., Peisach, J. & Horwitz, S. B. Effect of chelating-agents and metal-ions on degradation of DNA by bleomycin. *Biochemistry* 17, 2740-2746 (1978).
35. Sausville, E. A., Peisach, J. & Horwitz, S. B. Role for ferrous ion and oxygen in degradation of DNA by bleomycin. *Biochem. Biophys. Res. Commun.* 73, 814-822 (1976).
36. Sausville, E. A., Stein, R. W., Peisach, J. & Horwitz, S. B. Properties and products of degradation of DNA by bleomycin and iron(II). *Biochemistry* 17, 2746-2754 (1978).
37. Oppenheimer, N. J., Rodriguez, L. O. & Hecht, S. M. Proton nuclear magnetic-resonance study of the structure of bleomycin and the zinc-bleomycin complex. *Biochemistry* 18, 3439-3445 (1979).
38. Akkerman, M. A. J., Haasnoot, C. A. G., Pandit, U. K. & Hilbers, C. W. Complete assignment of the C-13 NMR-spectra of bleomycin-A2 and its zinc complex by means of two-dimensional NMR-spectroscopy. *Magn. Reson. Chem.* 26, 793-802 (1988).
39. Keck, M. V., Manderville, R. A. & Hecht, S. M. Chemical and structural characterization of the interaction of bleomycin A(2) with d(CGCGAATTCGCG)(2). Efficient, double-strand DNA cleavage accessible without structural reorganization. *J. Am. Chem. Soc.* 123, 8690-8700 (2001).
40. Ehrenfeld Manderville, R. A., Ellena, J. F. & Hecht, S. M. Solution strucutre of a Zn(II)center-dot-bleomycin A(5)-d(CGCTAGCG)(2) complex. *J. Am. Chem. Soc.* 116, 10851-10852 (1994).
41. Sucheck, S. J., Ellena, J. F. & Hecht, S. M. Characterization of Zn(II)-deglycobleomycin A(2) and interaction with d(CGCTAGCG)(2): Direct evidence for minor groove binding of the bithiazole moiety. *J. Am. Chem. Soc.* 120, 7450-7460 (1998).
42. Ehrenfeld, G. M., Rodriguez, L. O., Hecht, S. M., Chang, C., Basus, V. J., & Oppenheimer, N. J. Copper(I)-bleomycin - structurally unique complex that mediates oxidative DNA strand scission. *Biochemistry* 24, 81-92 (1985).
43. Ehrenfeld, G. M., Shipley, J. B., Heimbrook, D. C., Sugiyama, H., Long, E. C., Vanboom, J. H., Vandermarel, G. A., Oppenheimer, N. J., & Hecht, S. M. Copper-dependent cleavage of DNA by bleomycin. *Biochemistry* 26, 931-942 (1987).
44. Hecht, S. M. Bleomycin: New perspectives on the mechanism of action. *J. Nat. Prod.* 63, 158-168 (2000).
45. Chien, M., Grollman, A. P. & Horwitz, S. B. Bleomycin-DNA interactions - fluorescence and proton magnetic-resonance studies. *Biochemistry* 16, 3641-3647(1977).
46. Berry, D. E., Chang, L. H. & Hecht, S. M. DNA damage and growth-inhibition in cultured human-cells by bleomycin congeners. *Biochemistry* 24, 3207-3214 (1985).
47. Booth, T. E., Sakai, T. T. & Glickson, J. D. Interaction of bleomycin-A2 with poly(deoxyadenylylthymidylic acid) - a proton nuclear magnetic-resonance study of the influence of temperature, pH, and ionic-strength. *Biochemistry* 22, 4211-4217 (1983).
48. Ohno, M. & Otsuka, M. in *Recent Progress in the Chemical Synthesis of Antibiotics* (eds G. Lukacs & M. Ohno) 387-414 (Springer 1990).

49. Schroeder, B. R., Ghare, M. I., Bhattacharya, C., Paul, R., Yu, Z. Q., Zaleski, P. A., Bozeman, T. C., Rishel, M. J., & Hecht, S. M. The disaccharide moiety of bleomycin facilitates uptake by cancer cells. *J. Am. Chem. Soc.* 136, 13641-13656 (2014).
50. Takita, T., Muraoka, Y., Nakatani, T., Fujii, A., Iitaka, Y., & Umezawa, H. Chemistry of bleomycin .21. Metal-complex of bleomycin and its implication for mechanism of bleomycin action. *J. Antibiot.* 31, 1073-1076 (1978).
51. Takeshita, M., Grollman, A. P., Ohtsubo, E. & Ohtsubo, H. Interaction of bleomycin with DNA. *Proc. Natl. Aca. Sci. USA* 75, 5983-5987 (1978).
52. D'Andrea, A. D. & Haseltine, W. A. Sequence specific cleavage of DNA by the antitumor antibiotics neocarzinostatin and bleomycin. *Proc. Natl. Aca. Sci. USA* 75, 3608-3612 (1978).
53. Burger, R. M., Drlica, K. & Birdsall, B. The DNA cleavage pathway of iron bleomycin - strand scission precedes deoxyribose 3-phosphate bond-cleavage. *J. Biol. Chem.* 269, 25978-25985 (1994).
54. McGall, G. H., Rabow, L. E., Ashley, G. W., Wu, S. H., Kozarich, J. W., & Stubbe, J. New insight into the mechanism of base propenal formation during bleomycin-mediated DNA-degradation. *J. Am. Chem. Soc.* 114, 4958-4967 (1992).